

# BEHAVIOUR OF REINFORCED BRICK MASONRY COLUMNS WITH DIFFERENT SLENDERNESS RATIOS

A. OHLER

Research engineer, University of Kaiserslautern, West Germany

## ABSTRACT

This paper reports on a large test series of laterally and vertically reinforced masonry columns subjected to axial compression. The deformation behaviours and bearing strengths of piers differing in types of bricks, mortars, reinforcements, and slenderness are investigated. The experimental results comprise the effect of the shapes of reinforcement, strength enhancements and load decreases due to slenderness. A design method is proposed taking into account the parameters investigated.

## 1. INTRODUCTION

Brickwork loaded in compression is subjected to a triaxial stress state. This stress state is different for the bricks and the mortar due to their different expansion behaviours: the mortar tends to expand laterally more than the brick thus inducing lateral tensile stresses on the brick. Since the brick acts as a confining material the mortar is subjected to lateral compressive stress. Failure occurs when the lateral tensile stress exceeds the tensile strength of the brick. Earlier research work [1] has shown that embedding horizontal reinforcement in the bed joints of brickwork piers is an effective means in terms of restraining the lateral expansion of the mortar. It yields a reduction of the tensile stresses induced in the brick and, consequently, an enhancement of the bearing capacity of the whole structure.

Since the publication of the investigation [1] results of which were presented at the 6th IBMaC at Rome, 1982, tests have been continued using more types of bricks, additional vertical reinforcements, and piers varying in heights and widths. Effects of the different shapes of reinforcements were quantified and formulae and coefficients were presented to predict the strengths of short and slender masonry piers.

## 2. TESTING PROGRAMME

### 2.1. Materials

Bricks used were sand-lime perforated bricks (abbreviation KS 2 DF, length/width/height = 240/115/113 mm) and perforated clay bricks (abbreviation P 2 DF, same dimensions). Standard compression tests were conducted in accordance with the German standards DIN 105 and 106 [2]. Results are shown in Table 1.

Two types of mortar were used being type IIa a hydraulic-lime-cement mixture and type III a portland-cement mixture. Standard compression and flexural tensile tests of the 40/40/160 mm cubes complied with the German standard DIN 1164 [3]. Results are shown in Table 2.

| type of brick                           | German abbreviation           | Average compressive strength<br>[N/mm <sup>2</sup> ] | brick used in piers No.  |
|---|-------------------------------|--|--|
| perforated clay brick<br>(P 2 DF)       | H1Z<br>0,8/6/2DF<br>DIN 105   | 7,98   | P 19 ... P 25<br>P 37 ... P 40                                   |
| perforated sand-lime brick<br>(KS 2 DF) | KS1<br>1,4/12/2 DF<br>DIN 106 | 14,46<br>20,65<br>16,09                              | KS 30 ... KS 34<br>KS 45, KS 47<br>KS 46, KS 50,<br>KS 51, KS 52 |

Table 1 Characteristics of bricks

| mortar group | mortar mix by weight<br>cement: masonry-cement: sand | $\frac{\text{water}}{\text{cement}}$ ratio | average compressive strength<br>[N/mm <sup>2</sup> ] | average flexural tensile strength<br>[N/mm <sup>2</sup> ] |
|--------------|--|--|--|---|
| IIa          | 1 : 2 : 8  | 0,41                                       | 10,1   | 2,47  |
| III          | 1 : 0 : 4  | 0,50                                       | 20,8   | 2,76  |

Table 2 Characteristics of mortars

Since earlier tests [1] had shown that square hoops were ineffective in terms of strength enhancement only two shapes of reinforcement were used (fig. 1): a wire mesh  $\emptyset$  3 mm commonly used in reinforced concrete structure and a round hoop consisting of a steel bar  $\emptyset$  6 mm which was carefully welded together on both ends. According to the cross sections chosen to construct the masonry piers (fig. 2) two sizes of the lateral bed-joint reinforcement were needed.

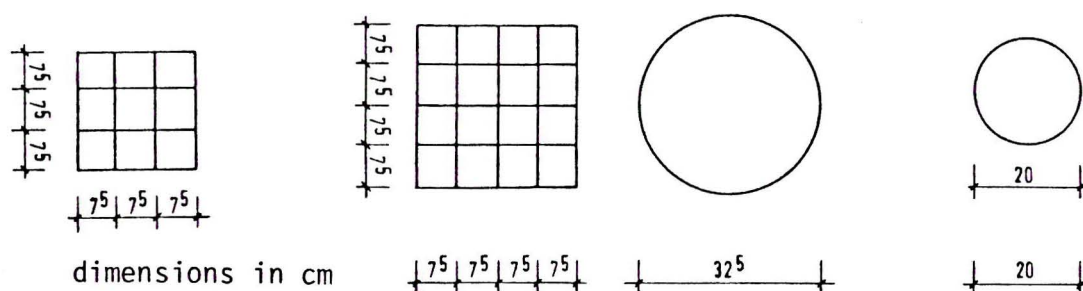


Fig. 1 Shape of horizontal reinforcements

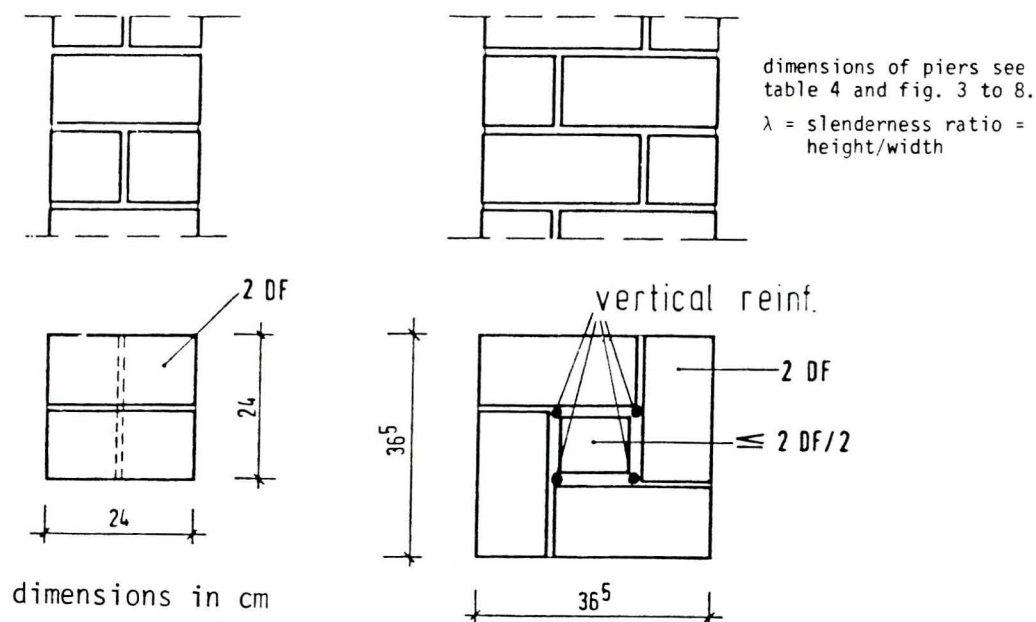


Fig. 2 Section and elevation of piers tested

## 2.2. Specimens

Due to the results obtained in the first part of the test series [1] not all possible combinations of the types of bricks, mortars and reinforcements were investigated. Variations of the parameters chosen for the tests can be obtained from Table 4. All specimens consistently had a joint thickness of 12 mm. After completion they were capped with a thin layer of gypsum to provide an even and parallel surface. They were cured for 28 to 29 days in a laboratory where the temperature was maintained between 10 to 17° Celsius and the relative humidity between 50 and 70 %. Strains were measured vertically spanning over 1 or 4 joints, horizontally spanning over one vertical joint or just transversing the brick.

All piers were tested in accordance with the German standard DIN 18 554 [4]. Load was applied axially in equal increments, and the load was held constant while strain readings were taken. To determine the plastic deformations of the piers under working stress conditions the specimens were subjected to cyclic loading five times up to about 40 % of the expected ultimate load. Then, the 6th loading was conducted till failure.

## 3. TEST RESULTS

### 3.1. Mode of failure

As was the case for the piers tested in [1] two major failure modes were recorded: All short unreinforced piers splitted vertically along the joints and straight through the bricks. The laterally reinforced piers showed local spalling of the bricks which was distributed unregularly over the complete height of the specimen. Due to buckling of the inner column formed by the four vertical reinforcing bars and the brick core (fig. 2) the vertically reinforced piers exhibited an even more "explosive" crush when failure load was approached. Piers having additional lateral hoops showed a failure pattern similar to that of the reinforced specimens without vertical bars. But the relatively weak brick bond of the 365/365 mm specimens was less effective in terms of lateral expansion than that of the 240/240 mm cross section piers and therefore

tended to break up at higher loads. The horizontal reinforcement was not able to prevent this phenomenon.

All slender columns tested ( $\lambda = 11,46; 16,15$ ) failed in buckling; failure produced a nearly complete destruction of the cross section at which crushing was led off while other parts of the column were unharmed. This was the case for all reinforced and unreinforced specimens, the latter showing slightly more gaping cracks. Fig. 9 shows typical failure patterns of the piers tested.

### 3.2. Stress-strain-relationships

The stress-strain-curves (fig. 3 to 9) confirm the theoretically assumed strangling effect of the horizontal reinforcement: in most cases the reinforced piers exhibit a steeper inclination and a greater radius of curvature in the upper range of the stress-vertical strain-curves than did the unreinforced piers. The lateral expansion curves of the unreinforced piers show significant strain increases in the upper third of the loading range. The reinforcement provides a strain reduction in this area and straightens the curve as a whole thus delaying or even cancelling the critical phase where micro-cracks begin to lead off the failure procedure. In the case of the slender columns the load deflection curves do not reach this "cracking zone" due to the fact that buckling occurs before the compressive strength of the pier can fully be exploited. Nevertheless the reinforcement does cause a strain reduction at comparable strengths yielding significant load enhancements.

## 4. DISCUSSION OF TEST RESULTS

Ultimate loads, strengths and important strain readings are listed in Table 4. The strains monitored prior to final loading represent the maximum lateral and vertical deflections of the specimens after cyclic loadings within the working stress. The values obtained - about 0.02 % for lateral and 0.06 % for vertical strains - were found constant after 4 to 5 loading cycles. They appear to be slightly influenced by the type of brick rather than the shape of reinforcement. Since reinforcement is effective when higher stress states are reached lateral hoops or wire meshes do not affect the plastic deformations caused by load cycles within the working stress.

Load enhancements due to the use of bed joint reinforcements are up to 33 % not dependent on the shape of the cross section used (see fig. 2). The maximum values are obtained with short piers because the full compressive strength of the specimen is exploited. For slender columns failure is determined by buckling and, hence, the load increase caused by the hoops and wire mesh only comes up to 24 %. The effect of the bed joint reinforcement is based on the fact that the mortar which tends to expand laterally under vertical compressive stress is subject to a constraint due to strangling forces induced by the reinforcement. This effect, of course, cannot be provided by vertical reinforcing bars, but considering the results of [5,6] the test carried out with this type of reinforcement aimed to find out if the vertical load applied could be taken by the masonry and, to a certain extent, by the reinforcement. Further calculations based on strain readings (for more details see [7]) show that a maximum of 10 % of the whole compressive stress was taken by the reinforcing bars. Together with the inner brick core surrounded by them the bars form a slender column within the 365 mm cross section of the pier so that when the ultimate load is approached failure is due to buckling of this inner column rather than exceeding the compressive stress of the brickwork. As a conclusion, vertical reinforcement used in the way tested herein is considered to be ineffective.

## 5. STRENGTH PREDICTION

### 5.1. Short piers without buckling

Statistical regression analyses were carried out to describe the stress-strain diagrammes mathematically. On the basis of analytical calculations of the deformation work stresses  $\sigma_{rm}$  were calculated which, for each pier, represent the beginning of the failure comparable to the crack load (for more details see [7]). Statistical consideration of all short piers reported herein and in [1] yielded the expression

$$\sigma_{Br} = \frac{z_m}{\varphi} \sqrt{\frac{\beta_{st}}{c/1000}} \quad (1)$$

where

$\sigma_{Br}$  = failure strength of an unreinforced or reinforced masonry pier

$z_m$  = coefficient representing the type of mortar and shape of reinforcement (table 3)

$\varphi$  = coefficient representing the difference between crack load and ultimate load (table 3)

$\beta_{st}$  = compressive strength of brick according to the German standard compression test ([2])

$c$  = coefficient representing the type of brick  
lightweight concrete blocks:  $c = 610$   
perforated clay bricks:  $c = 380$   
perforated sand-lime bricks:  $c = 300$

Equation (1) predicts the ultimate strength of short laterally reinforced masonry piers as a function of brick strength, type of brick, type of mortar, and shape of reinforcement, respectively.

A comparison of strengths computed with equ. (1) and experimental results published in [5,6,8] showed a good agreement.

### 5.2. Strength reduction due to buckling

Evaluating the tests carried out on slender columns (test group sand-lime bricks - mortar III) decreasing strengths with increasing slenderness ratios were recorded. To check the experimentally obtained results a computer programme was applied taking into account the non-linear deformation laws of the brickwork piers. For an assumed initial excentricity of length/1000, good agreement was obtained between experimental and theoretical failure loads. To determine the strength reduction as a function of the actual slenderness ratio of a pier further evaluations lead to a ln-function expressing the pier strength in reference to the brick strength and a certain "limit slenderness ratio". Being different for each shape of reinforcement this value was defined as to divide the ranges of

| shape of reinf. | type of mortar | $z_m$<br>[ $\sqrt{N/mm^2}$ ] | $\varphi$ |
|-----------------|----------------|------------------------------|-----------|
| no reinf.       | II a           | 0,783                        | 0,592     |
|                 | III            | 0,89                         |           |
| wire mesh       | II a           | 0,941                        | 0,592     |
|                 | III            | 1,032                        |           |
| round hoop      | II a           | 0,941                        | 0,684     |
|                 | III            | 1,177                        |           |

Table 3 Coefficients  $z_m$  and  $\varphi$

slenderness ratios where the strength of the structure is determined by failure with or without the influence of stability. The limit slenderness ratios  $\lambda_{\text{grenz}}$  were found to be greater for horizontal round hoops than for wire mesh and unreinforced piers. Referring either to short reinforced piers or, more generally, to a short unreinforced pier with the brick-mortar combination KS-MG III the following reduction factors were established:

$$c_{\lambda} = e^{m_i (\lambda_{\text{grenz}} - \lambda)} \quad (2)$$

$$c_{\lambda}' = e^{k - m_i \lambda} \quad (3)$$

where

$\lambda_{\text{grenz}}$  = limit slenderness ratio of each shape of reinforcement

$k, m_i$  = coefficients expressing the strength decreases with increasing slenderness ratios (for more details see [7])

Fig (10,11) show the slenderness coefficients  $c_{\lambda}, c_{\lambda}'$  as a function of the slenderness ratio  $\lambda$  of a pier. The graphs demonstrate that the actual German standard DIN 1053, part 1, does not well approximate the tests results obtained so that designing a pier in accordance with the standard by far overestimates the strength reduction due to buckling.

To predict the bearing capacity of a pier having slenderness ratios greater than the limits given in fig. (10,11) formula (1) can be used multiplied by the coefficients  $c_{\lambda}$  or  $c_{\lambda}'$ .

## 6. CONCLUSIONS

1. Embedding lateral reinforcement, such as round hoops or wire meshes, in the bed joint mortar is a suitable means for enhancing the bearing capacity of a brick masonry pier. Due to restraint of the lateral expansion of the mortar the tensile stress acting in the brick is reduced yielding strength increases of 33 % (short piers,  $\lambda = 4,79$ ) and 23 % (slender columns,  $\lambda = 16,15$ ).
2. Vertical reinforcement is nearly inefficient in terms of strength enhancement.
3. Based on the evaluation of test results presented herein and in an earlier investigation [1] equation (1) was found which predicts the ultimate strength of a masonry pier as a function of type and compressive strength of brick, type of mortar, and shape of lateral reinforcement, respectively.
4. Failure load decreases with increasing slenderness ratios of the piers tested were found to be in disaccordance with the requirements of the German standard DIN 1053, part 1. For the test group sand-lime bricks/mortar III coefficients (2) and (3) were derived expressing the influence of slenderness in reference to the strength of short reinforced or unreinforced piers.

## 7. REFERENCES

- [1] OHLER/GÖPFERT "The Effect of Lateral Joint Reinforcement on the Strength and Deformation of Brickwork Piers". Proceedings of the 6th IBMaC, Rome, 1982.
- [2] DIN 105 "Mauerziegel" (German standard)  
DIN 106 "Kalksandsteine" (German standard)
- [3] DIN 1164 "Teil 7, Portland-, Eisenportland-, Hochofen- und Traßzement, Bestimmung der Festigkeit" (German standard)
- [4] DIN 18 554 "Mauerwerk - Ermittlung der Tragfähigkeit von Wänden und Pfeilern" (German standard)
- [5] LYSE, J. "Tests of Reinforced Brick Columns".  
Journal of the American Ceramic Society, Vol 16, 1933
- [6] WITHEY, M. "Tests on Reinforced Brick Masonry Columns".  
ASTM Proceedings, 1934
- [7] OHLER, A. "Tragfähigkeit und Bemessung von mittig gedrückten bewehrten Mauerwerkspfeilern"  
Dissertation University of Kaiserslautern, 1984,  
also published as "Mitteilungen des Fachgebietes Statik der Hochbaukonstruktionen der Universität Kaiserslautern, Heft 3, 1984".
- [8] FLOHRER/  
HILSDORF "Enhanced Ductility of Masonry Loaded in Compression".  
Proceedings of the 6th IBMaC, Rome 1982.
- [9] DIN 1053 "Mauerwerk - Berechnung und Ausführung" (German standard)


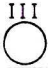
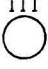

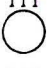


| pier No.                | type of mortar<br>type of reinf.   | $\lambda$<br>cross section dimensions<br>[cm/cm] | failure load<br>[kN] | strength<br>$\sigma_{ult}$<br>[ $\frac{kN}{cm^2}$ ] | $\frac{\sigma_{ult}}{\sigma_{ult, no reinf.}}$ | strains after cyclic loading      |                                   |                                   |                                   | ultimate strain measured        |                                |
|-------------------------|--|--|----------------------|---|--|-----------------------------------|-----------------------------------|-----------------------------------|-----------------------------------|---------------------------------|--------------------------------|
|                         |  |  |                      |   |  | min max<br>$\epsilon_{ol}$<br>[%] | average<br>$\epsilon_{ol}$<br>[%] | min max<br>$\epsilon_{oq}$<br>[%] | average<br>$\epsilon_{oq}$<br>[%] | vertical<br>$\epsilon_l$<br>[%] | lateral<br>$\epsilon_q$<br>[%] |
| P 19 <sup>a</sup><br>b  | II a<br>no reinf.  | 7,29<br>24/24                                    | 399,0<br>337,3       | 0,64  | 1,00   | 0,004<br>0,011                    | 0,008                             | 0,023<br>0,080                    | 0,054                             | 1,342                           | 1,502                          |
| P 20 <sup>a</sup><br>b  | II a<br>mesh   | 7,29<br>24/24                                    | 349,7<br>331,2       | 0,59  | 0,92   | 0,026<br>0,083                    | 0,055                             | 0,022<br>0,040                    | 0,031                             | 2,347                           | 1,420                          |
| P 21 <sup>a</sup><br>b  | II a<br>  | 7,29<br>24/24                                    | 354,6<br>321,3       | 0,59  | 0,92   | 0,050<br>0,072                    | 0,061                             | 0,003<br>0,019                    | 0,011                             | 1,670                           | 0,494                          |
| P 23 <sup>a</sup><br>b  | III<br>no reinf.   | 7,29<br>24/24                                    | 409,3<br>382,6       | 0,69  | 1,0  | 0,002<br>0,002                    | 0,002                             | 0,016<br>0,017                    | 0,017                             | 1,170                           | 0,657                          |
| P 24 <sup>a</sup><br>b  | III<br>mesh  | 7,29<br>24/24                                    | 444,3<br>482,6       | 0,81  | 1,17   | 0,014<br>0,022                    | 0,018                             | 0,022<br>0,039                    | 0,031                             | 1,448                           | 0,522                          |
| P 25 <sup>a</sup><br>b  | III<br>   | 7,29<br>24/24                                    | 399,0<br>491,2       | 0,77  | 1,13   | 0,002<br>0,012                    | 0,007                             | 0,006<br>0,006                    | 0,006                             | 0,902                           | 0,217                          |
| KS 30 <sup>a</sup><br>b | III<br>no reinf.   | 4,79<br>36 <sup>s</sup> /36 <sup>s</sup>         | 1131,3<br>1189,9     | 0,87  | 1,0  | 0,038<br>0,039                    | 0,039                             | 0,012<br>0,024                    | 0,018                             | 1,781                           | 0,800                          |
| KS 31 <sup>a</sup><br>b | III<br>mesh  | 4,79<br>36 <sup>s</sup> /36 <sup>s</sup>         | 1378,2<br>1407,0     | 1,05  | 1,20   | 0,002<br>0,003                    | 0,003                             | 0,038<br>0,062                    | 0,050                             | 1,763                           | 0,600                          |
| KS 32 <sup>a</sup><br>b | III<br>  | 4,79<br>36 <sup>s</sup> /36 <sup>s</sup>         | 1530,4<br>1559,2     | 1,16  | 1,33   | 0,030<br>0,041                    | 0,036                             | 0,011<br>0,020                    | 0,016                             | 2,201                           | 1,307                          |
| KS 33 <sup>a</sup><br>b | III<br>::  | 4,79<br>36 <sup>s</sup> /36 <sup>s</sup>         | 1347,7<br>1415,2     | 1,04  | 1,19   | 0,038<br>0,043                    | 0,041                             | 0,029<br>0,033                    | 0,031                             | 2,011                           | 0,512                          |
| KS 34 <sup>a</sup><br>b | III<br> | 4,79<br>36 <sup>s</sup> /36 <sup>s</sup>         | 1193,0<br>1186,9     | 0,89  | 1,03   | 0,076<br>0,083                    | 0,080                             | 0,018<br>0,084                    | 0,051                             | 2,590                           | 1,119                          |
| P 37 <sup>a</sup><br>b  | III<br>no reinf.   | 4,79<br>36 <sup>s</sup> /36 <sup>s</sup>         | 1004,2<br>882,4      | 0,71  | 1,0  | 0,000<br>0,003                    | 0,002                             | 0,009<br>0,031                    | 0,020                             | 1,352                           | 0,394                          |
| P 38 <sup>a</sup><br>b  | III<br>mesh  | 4,79<br>36 <sup>s</sup> /36 <sup>s</sup>         | 975,0<br>1034,7      | 0,75  | 1,07   | 0,004<br>0,009                    | 0,007                             | 0,006<br>0,010                    | 0,008                             | 1,892                           | 0,563                          |
| P 39 <sup>a</sup><br>b  | III<br> | 4,79<br>36 <sup>s</sup> /36 <sup>s</sup>         | 1164,2<br>1160,1     | 0,87  | 1,23   | 0,002<br>0,003                    | 0,003                             | 0,005<br>0,018                    | 0,012                             | 1,512                           | 0,543                          |
| P 40 <sup>a</sup><br>b  | III<br>::  | 4,79<br>36 <sup>s</sup> /36 <sup>s</sup>         | 802,6<br>876,3       | 0,63  | 0,89   | 0,002<br>0,009                    | 0,006                             | 0,019<br>0,026                    | 0,023                             | 1,234                           | 0,610                          |
| KS 45 <sup>a</sup><br>b | III<br>no reinf.   | 11,46<br>24/24                                   | 680,9<br>634,4       | 1,14  | 1,0  | 0,022<br>0,029                    | 0,026                             | 0,005<br>0,009                    | 0,007                             | 1,408                           | 0,310                          |
| KS 46 <sup>a</sup><br>b | III<br>mesh  | 11,46<br>24/24                                   | 637,7<br>652,1       | 1,12  | -  | 0,040<br>0,046                    | 0,043                             | 0,009<br>0,010                    | 0,010                             | 1,587                           | 0,446                          |
| KS 47 <sup>a</sup><br>b | III<br> | 11,46<br>24/24                                   | 814,5<br>802,2       | 1,40  | 1,23   | 0,036<br>0,063                    | 0,050                             | 0,006<br>0,009                    | 0,008                             | 1,322                           | 0,254                          |
| KS 50 <sup>a</sup><br>b | III<br>no reinf.   | 16,15<br>24/24                                   | 499,8<br>464,9       | 0,84  | 1,0  | 0,034<br>0,066                    | 0,050                             | 0,006<br>0,011                    | 0,009                             | 1,661                           | 0,261                          |
| KS 51 <sup>a</sup><br>b | III<br>mesh  | 16,15<br>24/24                                   | 569,4<br>541,0       | 0,96  | 1,15   | 0,039<br>0,054                    | 0,047                             | 0,002<br>0,007                    | 0,005                             | 1,847                           | 0,409                          |
| KS 52 <sup>a</sup><br>b | III<br> | 16,15<br>24/24                                   | 610,1<br>572,2       | 1,03  | 1,23   | 0,049<br>0,050                    | 0,050                             | 0,003<br>0,009                    | 0,006                             | 1,819                           | 0,277                          |

Table 4 Test results

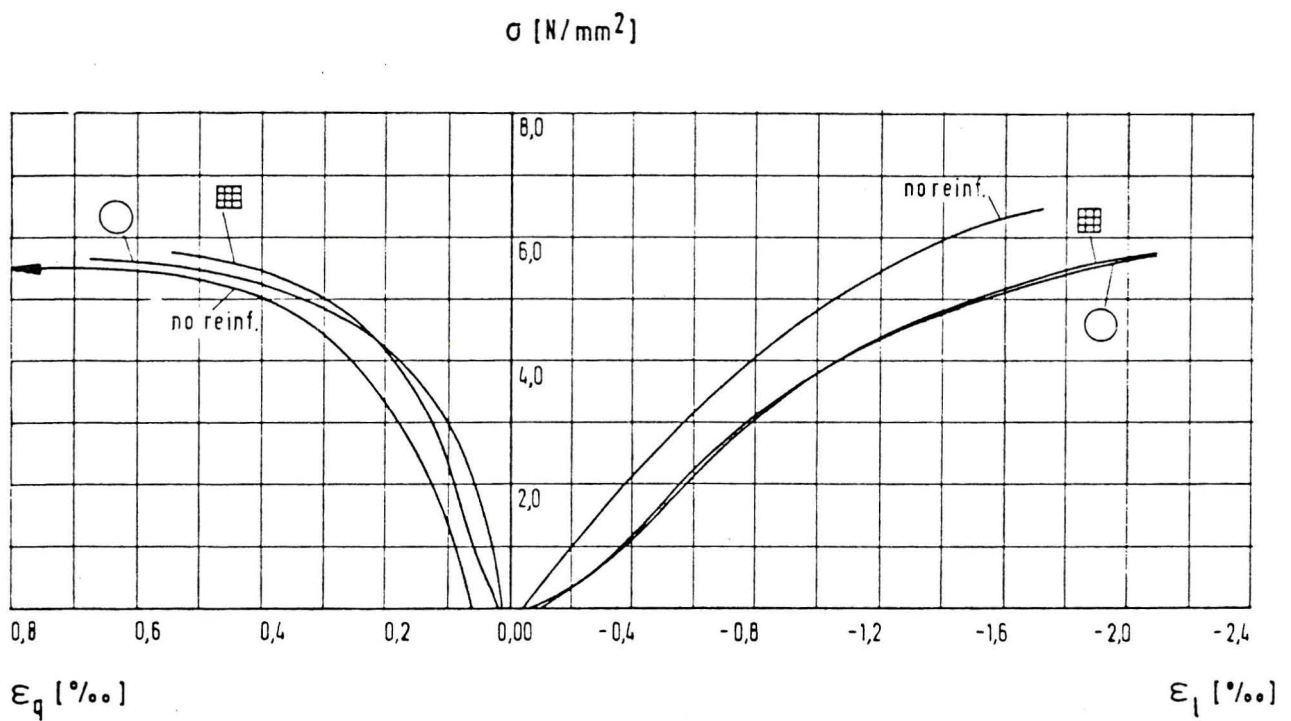


Fig. 3 Stress-strain-diagramme  
(Nr. P 19-21, MG IIa,  $\lambda = 175/24 = 7,29$ )

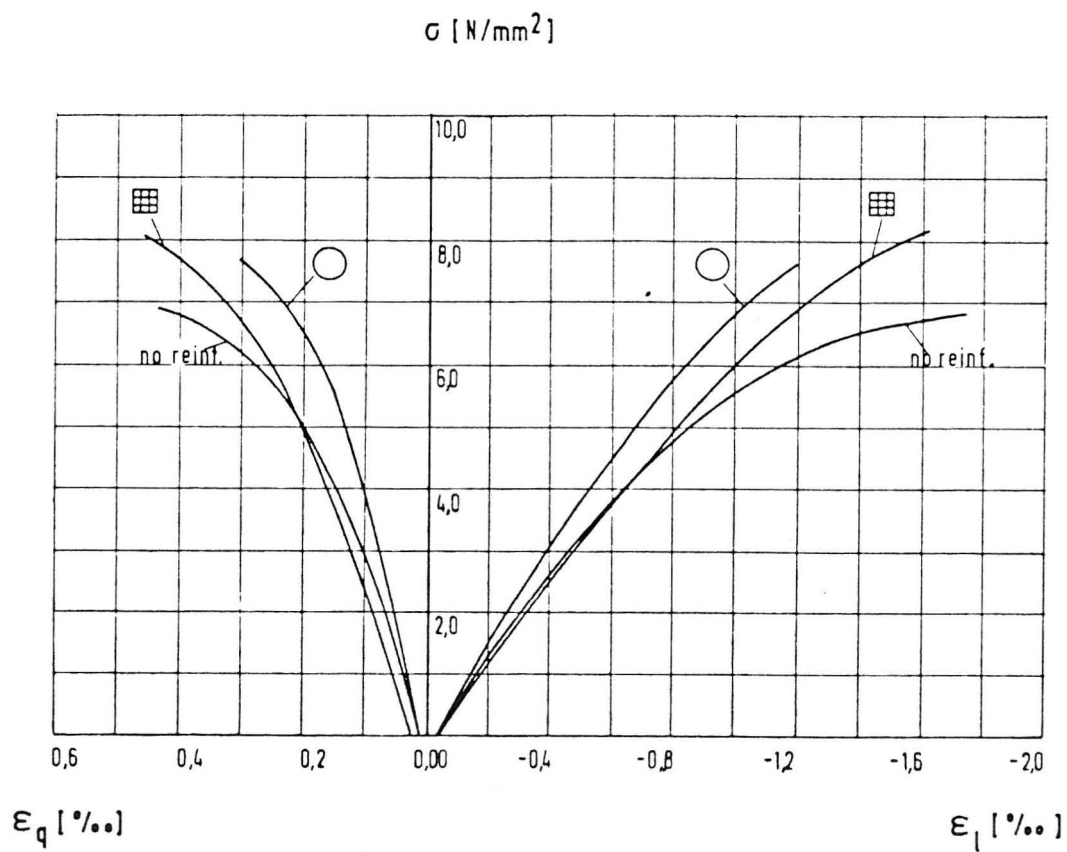


Fig. 4 Stress-strain-diagramme  
(Nr. P 23-25, MG III,  $\lambda = 175/24 = 7,29$ )

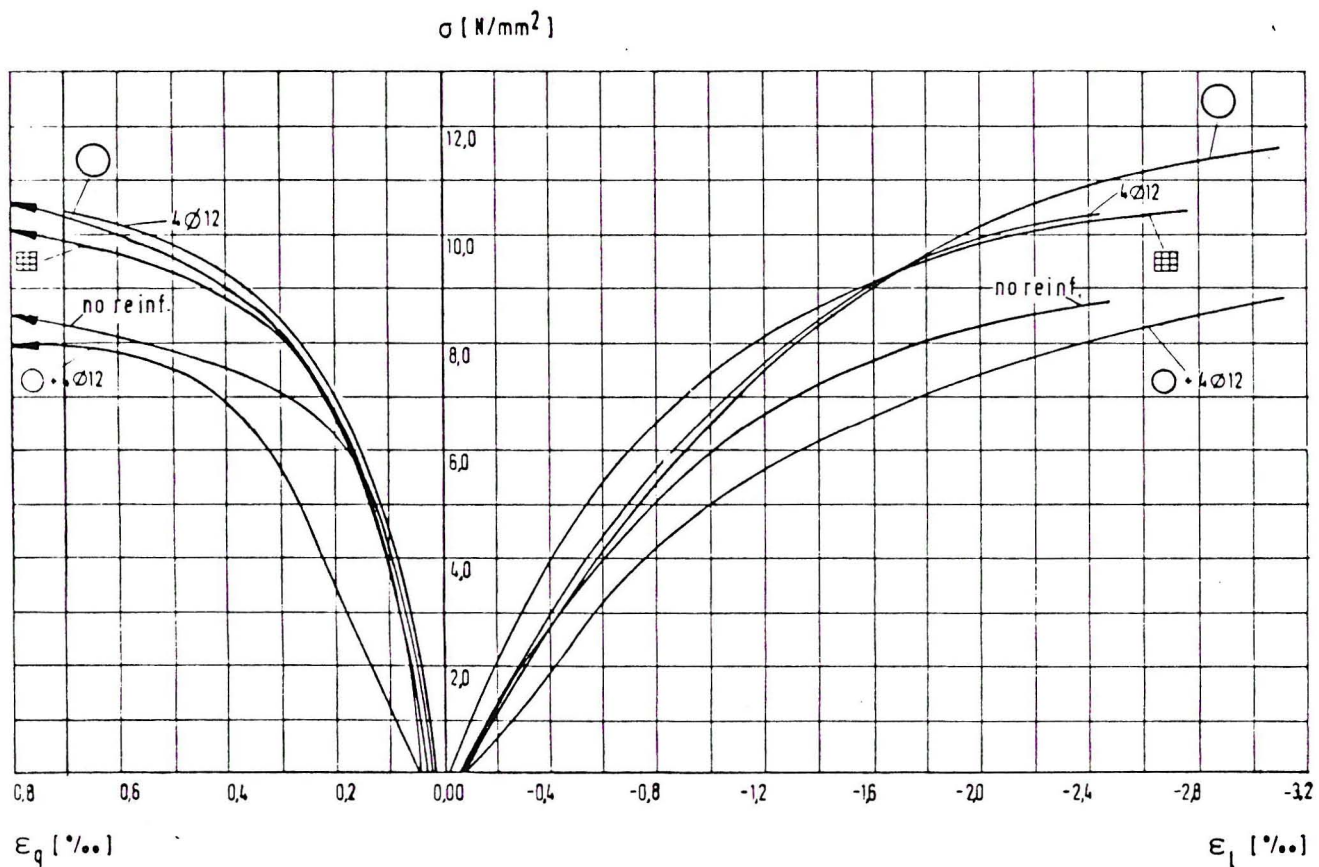


Fig. 5 Stress-strain-diagramme  
(Nr. KS 30-34, MG III,  $\lambda = 175/36,5 = 4,79$ )

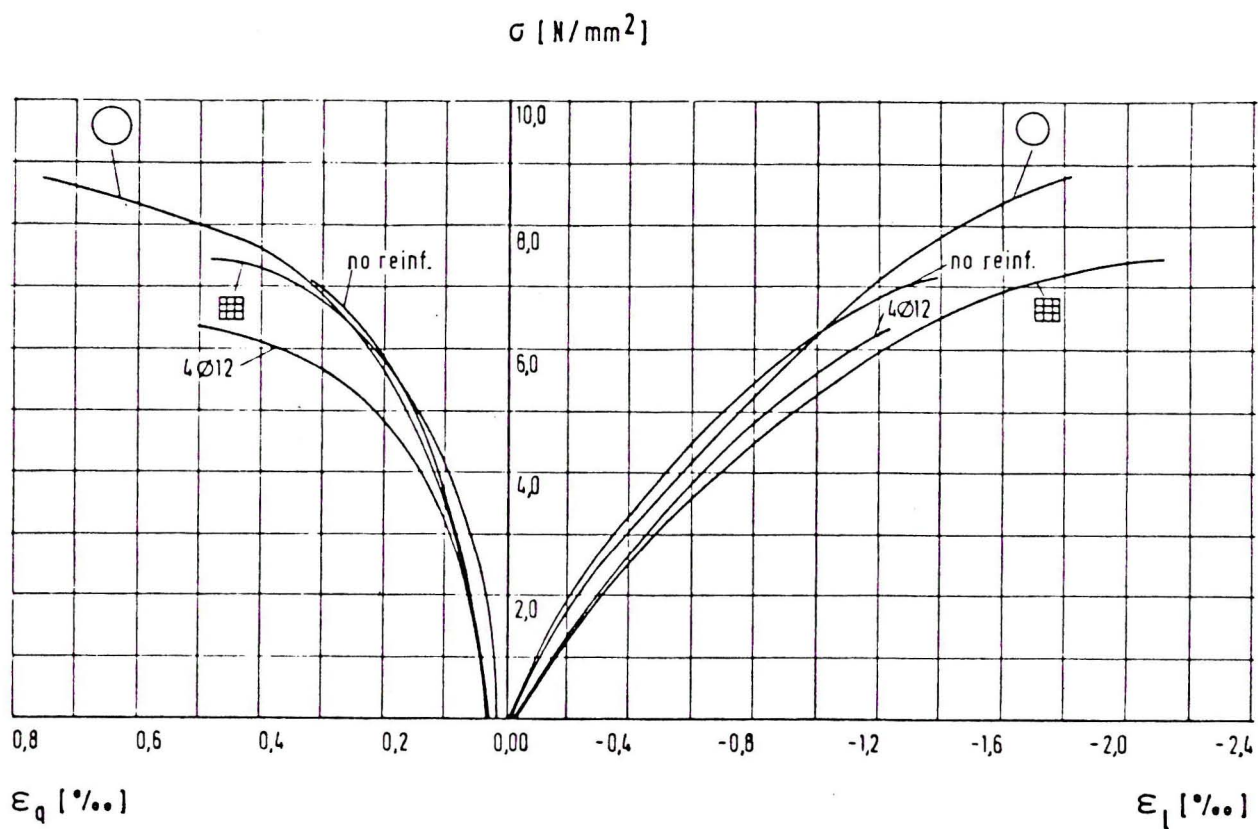


Fig. 6 Stress-strain-diagramme  
(Nr. P 37-40, MG III,  $\lambda = 175/36,5 = 4,79$ )

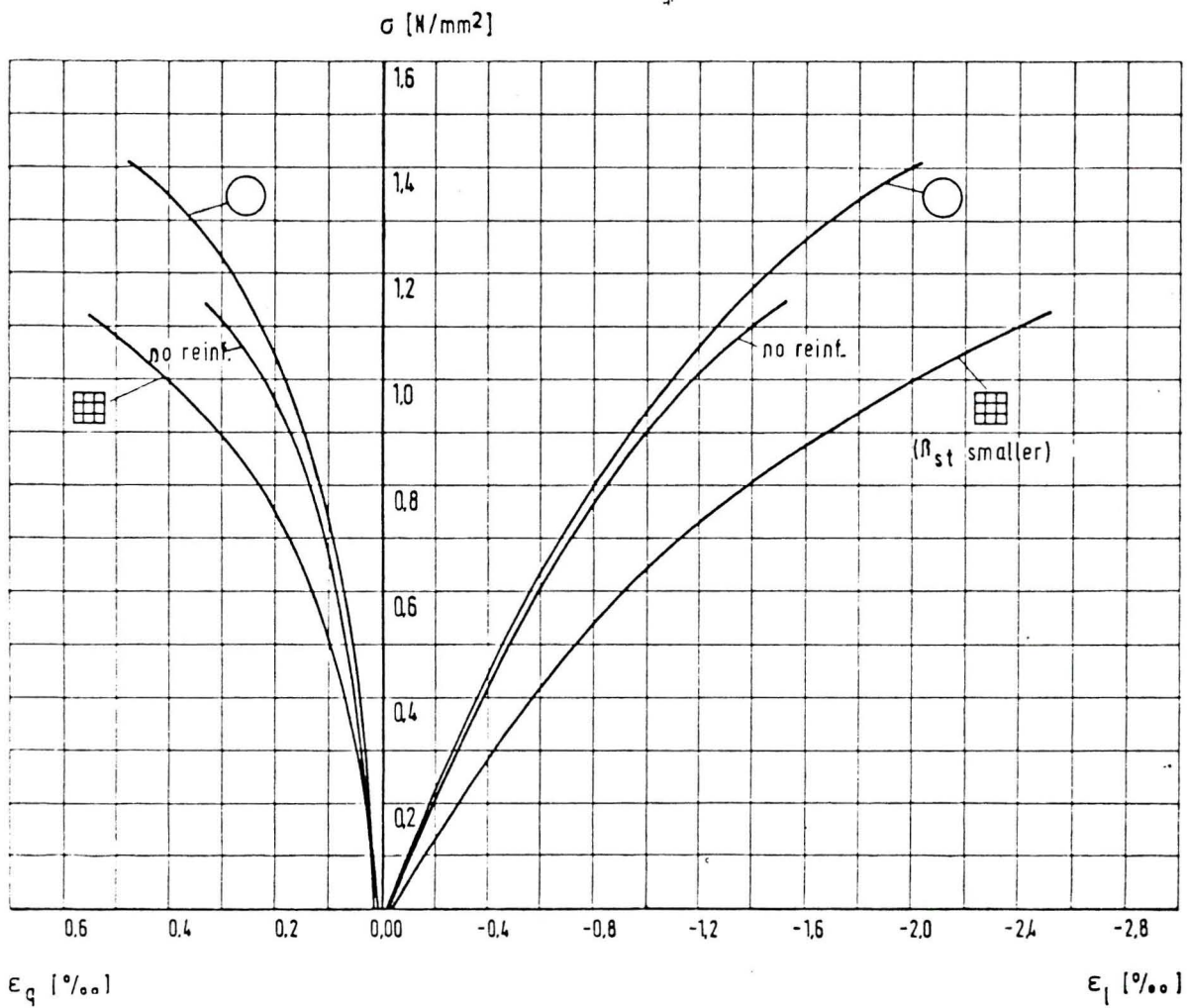
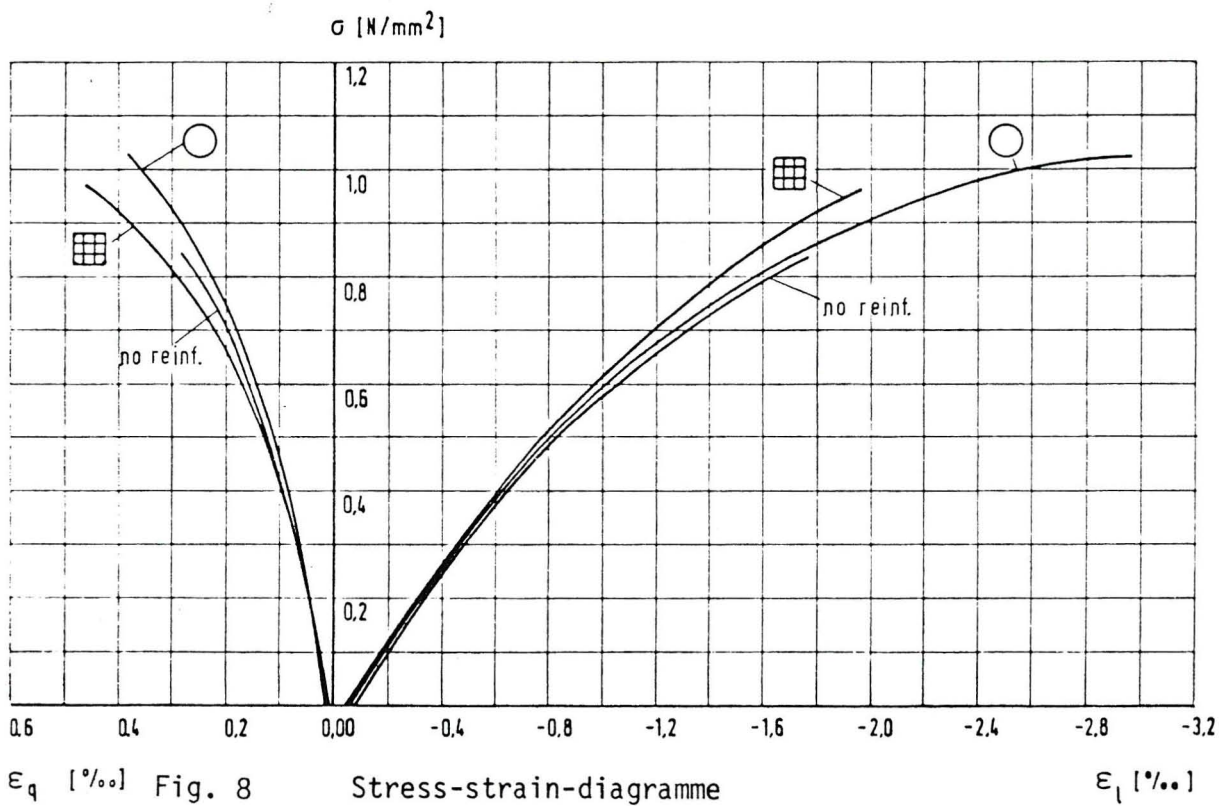


Fig. 7 Stress-strain-diagramme  
(Nr. KS 45-47, MG III,  $\lambda = 275/24 = 11,46$ )



Stress-strain-diagramme  
(Nr. KS 50-52, MG III,  $\lambda = 387,5/24 = 16,15$ )

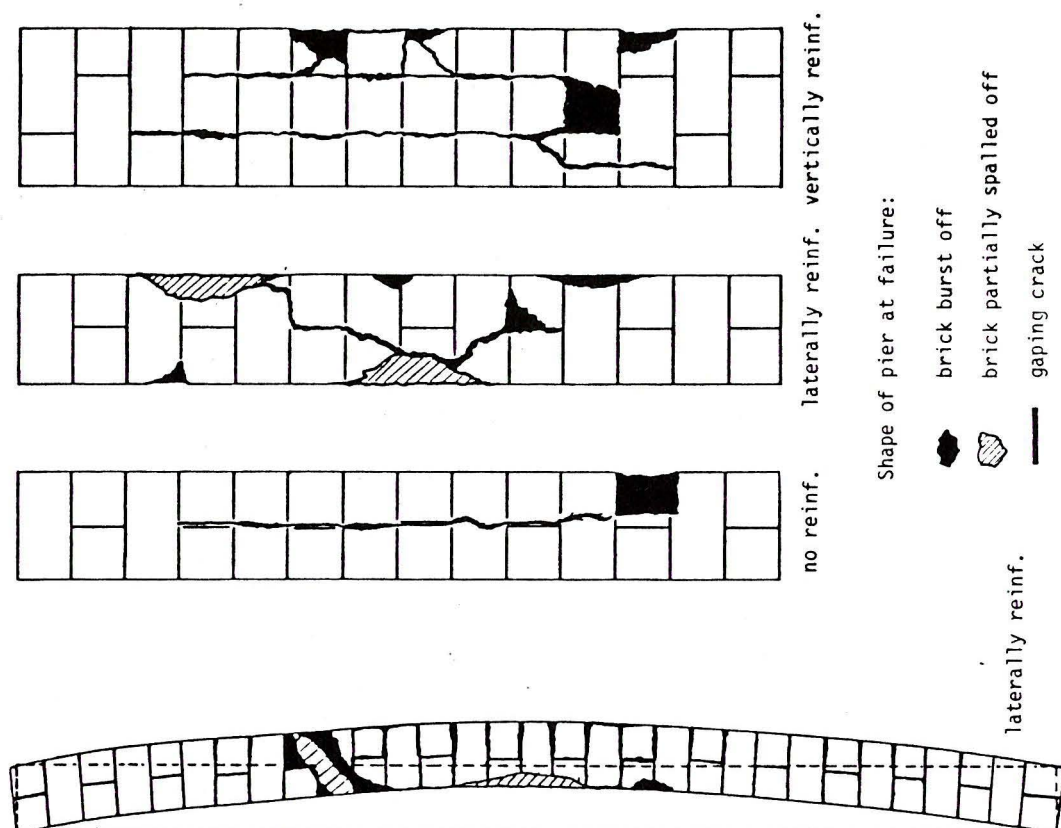


Fig. 9 Typical failure patterns

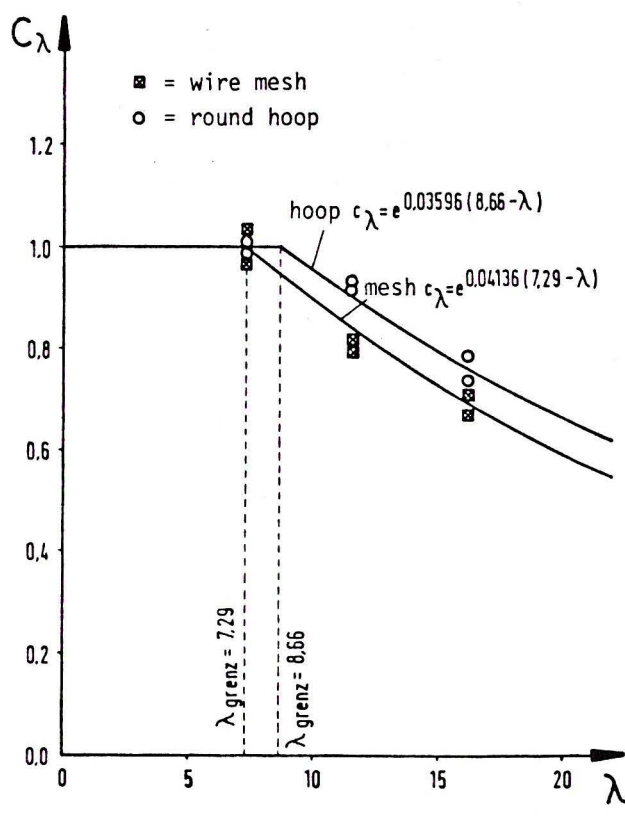


Fig. 10 slenderness coefficients  $c_\lambda = f(\lambda)$  referring to the reinforced piers

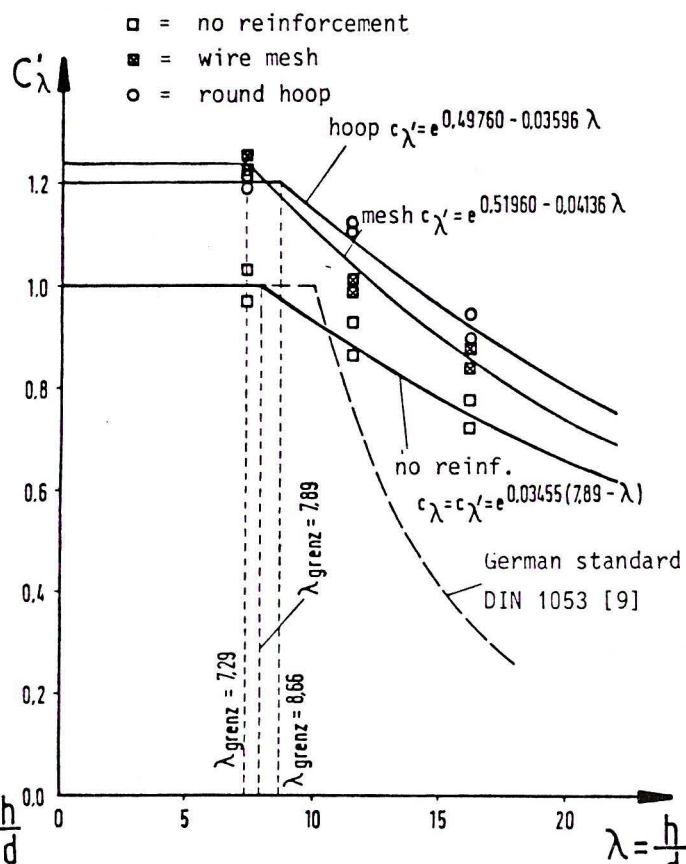


Fig. 11 slenderness coefficients  $c'_\lambda = f(\lambda)$  referring to the unreinforced pier